Journal of Advanced Research 53 (2023) 219–234

Contents lists available at ScienceDirect

Journal of Advanced Research

journal homepage: www.elsevier.com/locate/jare

Original Article

A single-cell transcriptomic landscape of mouse testicular aging

Wei Zhang [a,b,1], Siyu Xia [a,b,1], Wei Xiao [c,1], Yali Song [d,1], Li Tang [d], Min Cao [a,b], Jing Yang [a,b], Shuang Wang [a,b], Zhijie Li [a,b], Chengchao Xu [a,b], Jianqiao Liu [e,*], Shanchao Zhao [f,*], Chuanbin Yang [a,b,*], Jigang Wang [a,b,d,g,*]

[a] Department of Nephrology, and Shenzhen key Laboratory of Kidney Diseases, Shenzhen People's Hospital (The Second Clinical Medical College, Jinan University, The First Affiliated Hospital, Southern University of Science and Technology), Shenzhen 518020, China
[b] Shenzhen Clinical Research Centre for Geriatrics, Shenzhen People's Hospital, Shenzhen 518020, China
[c] Key Laboratory of Glucolipid Metabolic Disorder, Ministry of Education, Guangdong Pharmaceutical University, Guangzhou 510006, China
[d] Center for Reproductive Medicine, Dongguan Maternal and Child Health Care Hospital, Southern Medical University, Dongguan 523000, China
[e] Key Laboratory for Reproductive Medicine of Guangdong Province, the Third Affiliated Hospital of Guangzhou Medical University, Guangzhou 510150, China
[f] Department of Urology, the Third Affiliated Hospital of Southern Medical University, and Nanfang Hospital, Southern Medical University, Guangzhou, 510500, China
[g] Artemisinin Research Center, and Institute of Chinese Materia Medica, China Academy of Chinese Medical Sciences, Beijing 100700, China

HIGHLIGHTS

- The first single-cell transcriptomic atlases of testes of young and old mice were constructed.
- Revealed aging-associated heterogenous differentially expressed genes in mouse testes.
- Discovered aging-associated dysregulation of multiple biological processes in mouse testes.
- Aging disrupted balance of undifferentiated and differentiated spermatogonia stem cells in spermatogonia.
- Aging increased a subtype of aging-specific macrophages.

GRAPHICAL ABSTRACT

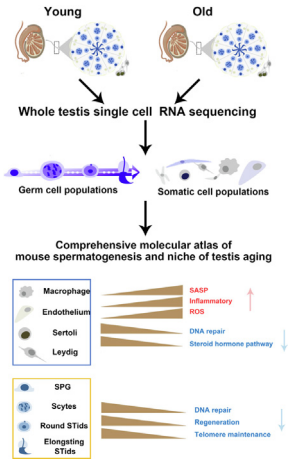

ARTICLE INFO

Article history:
Received 21 May 2022
Revised 8 December 2022
Accepted 11 December 2022
Available online 14 December 2022

ABSTRACT

Introduction: Advanced paternal age of reproduction is an increasing trend, especially in developed countries and areas. This trend results in elevated risks of adverse reproductive outcomes such as reduced fertility rates, increased pregnancy loss, and poor childhood health. Yet, a systematic profiling of aging-associated molecular and cellular alterations in testicular tissue is still missing.
Objectives: We aimed to dissect aging-associated molecular characteristics in testes of mice.

Abbreviations: DEGs, Differentially expressed genes; PCNA, proliferating cell nuclear antigen; ScRNA-seq, single-cell RNA sequencing; ROS, Reactive Oxygen Species; FC, Fold Change.

Peer review under responsibility of Cairo University.

* Corresponding authors at: Department of Nephrology, and Shenzhen key Laboratory of Kidney Diseases, Shenzhen People's Hospital (The Second Clinical Medical College, Jinan University, The First Affiliated Hospital, Southern University of Science and Technology), Shenzhen 518020, China (C. Yang and J. Wang); Department of Urology, the Third Affiliated Hospital of Southern Medical University, Guangzhou, 510500, China (S. Zhao); Key Laboratory for Reproductive Medicine of Guangdong Province, the Third Affiliated Hospital of Guangzhou Medical University, Guangzhou 510150, China (J. Liu).
E-mail addresses: liujqssz@gzhmu.edu.cn (J. Liu), lulululu@smu.edu.cn (S. Zhao), h1094103@connect.hku.hk (C. Yang), jgwang@icmm.ac.cn (J. Wang).
[1] These authors contributed equally to this work.

https://doi.org/10.1016/j.jare.2022.12.007

Keywords:
Aging
Testis
Single-cell RNA sequencing
Senescence
Inflammation

Methods: Single-cell transcriptomic sequencing and analysis were conducted in testes of young (2 months old) and old mice (24 months old). Immunofluorescences and immunochemistry were used to characterize aging-associated phenotypes and verify single cell sequence results.
Results: Here, we constructed the first single-cell transcriptomic atlases of testes of young and old mice. In-depth dissection of aging-dependent transcriptional alterations in specific cell types revealed multiple dysregulated biological processes such as increased 'senescence-associated secretory phenotype' and 'inflammation', which were major aging-associated characteristics. Further analysis of aging-related differentially expressed genes uncovered a disrupted balance of undifferentiated and differentiated spermatogonia stem cells in spermatogonia, indicative of a potential role of spermatogonia stem cells in aging-associated subfertility. Importantly, for the first time, our results identified an increased subtype of aging-specific macrophages, which may contribute to a hostile proinflammatory microenvironment during testicular aging.
Conclusion: Taken together, our findings depict the distinct single-cell transcriptional features of the aged mouse testes and provide enormous resources for a comprehensive understanding of the cell-type-specific molecular mechanisms underlying mouse testicular aging, which may shed light on developing novel potential diagnostic biomarkers and therapeutic targets for age-associated male subfertility.

Introduction

Aging is a conserved feature for living organisms including the single-celled budding yeast, mice, and humans [1–3]. It is a complex and pleiotropic biological process that affects multiple aspects of mammalian physiology, including reproductive development. The testis is a major reproductive organ that shows aging-associated dysfunction in humans, with reduced sperm quality and male fertility starting at around age 40 to 45 years [4]. Notably, there has been a significant increase in the delayed paternal age of reproduction in recent years, especially in high-income countries and areas. The increasing trend of advanced paternal age in modern societies results in the aging-associated decline in testicular functions. It not only affects the fertilizing capacity but also compromises the overall quality of life. For instance, delayed paternal age induces an increase in infertility rate, increases pregnancy loss, and causes poor childhood health outcomes. Importantly, testicular aging increases the risk of multiple age-related diseases such as cardiovascular diseases and certain cancers [5–7]. However, the underlying molecular mechanisms of testicular aging are not completely understood. As such, an in-depth and full understanding of testicular aging is of paramount importance.

Spermatogenesis is a complex process that produces mature sperms, which is crucial for male reproduction. It involves the differentiation of spermatogonia into spermatocytes in a step-wise manner and is coordinated by the interaction of multiple somatic cells and germ cells within the testis [8]. To determine the transcriptional alterations of aging-associated genes in the testis, previous studies mainly focused on certain cell types in the testis or relied on bulk RNA sequence data from aggregated RNA from various spermatogenic cell types [9] due to the difficulties in isolating specific cell types within the testis.

However, as a complex organ, the response of various cell types within the testis during aging is heterogeneous [10], and bulk-RNA sequencing analysis can not accurately reflect the information of specific cell types of testis during aging, indicating the necessity of employing advanced technology such as single-cell RNA sequencing (ScRNA-seq) approach to dissect the underlying mechanisms of testicular aging. Recently, ScRNA-seq technology has enabled the comprehensive determination of transcriptional sequence information of individual cells at the single-cell resolution, especially for assessing the transcriptional heterogeneity and uncovering the rare cell types or unknown dynamics of the cellular complexity during aging [11,12], allowing for a better understanding of the cellular differences and function of different cell types, especially for rare cell types in multiple organs including the testis. For instance, ScRNA-seq has advanced our understating of testis development [9,13–17], and our recent study revealed the endocrine disruptor bisphenol A-associated testicular injury [18].

Due to limited access to disease-free testicular tissues of humans, model organisms such as mice that have genetic and physiological similarities to humans, are widely used as alternative sources for studying the underlying mechanisms of the aging process. For instance, multiple organs of mice including the brain [19], liver [20], heart [21], ovarian [22], and other organs [23,24], have been used to investigate the aging process by ScRNA-seq, providing novel insight into our understanding of the aging process in diverse organs at a single-cell resolution. However, ScRNA-seq has not been yet applied to systematically and in-depth characterization of testicular aging in mouse.

Here, we establish a transcriptomic landscape of the testicular aging via advanced ScRNA-seq technology in mice. We revealed gene-expression signatures for eight testicular cell types and mapped the specific transcriptional landscape of testicular tissues during aging. Moreover, we identified several key features as hallmarks of testicular aging by examining the shared and cell-types-specific changes of genes, and pathways of each cell type within the testis during aging. Notably, we identified an increased subtype of proinflammatory macrophage, indicative of its potential role in contributing to the hostile inflammatory microenvironment during testicular aging. This study not only provides novel insight into our understanding of the underlying mechanisms of aging in the testis but also presents a valuable resource and foundation for additional discoveries of novel potential biomarkers and therapeutic targets against aging-related subfertility.

Methods

Animals

All C57BL/6 mice, ordered from 'Shanghai Model Organisms' in China, were housed under 12 light–dark cycles and provided with food and water ad libitum. Our research was carried out according to the Guidelines of the institution's Animal Care and Use Committee.

Immunofluorescence staining and immunochemistry staining

The testicular tissues embedded in Paraffin or OCT (N = 5, 6) were serially sliced into 4–10 μm sections and subjected to

immunofluorescence, or immunochemistry staining, with indicated primary antibodies or fluorescent secondary antibody/DAB (3,3′-diaminobenzidine) staining, as described previously [25,26]. Images were observed and captured with a microscope.

Preparation of single-cell suspension

Single-cell suspension was prepared according to a previous report [16]. In brief, seminiferous tubules from mouse testis were digested using Collagenase IA (Sigma), and DNase I (Thermo), followed by trypsinization. Single cells were then filtered through a 100 μm strainer, washed, and re-suspended in MACS buffer for Drop-Seq (10Xgenomics).

Single-cell libraries construction and sequencing

Drop-seq sequencing libraries were established as described previously [27]. Briefly, the single cells suspension and beads were mixed to co-encapsulation occupancy of 0.05. Individual droplets were harvested, and mRNA was reverse transcribed, followed by cDNA amplification. A 3′ gene expression library was constructed using a 10 × Genomics Chromium Single Cell system. Sequencing was performed on a NovaSeq 6000 (Illumina) by Novogene.

Read alignment and gene expression quantification

Reads were aligned to the mm10 reference genome of Ensembl. Gene annotations were derived from the GENCODEvM20. 10 × Genomics Cell Ranger 6.1.1 was employed to perform alignment, unique molecular identifiers (UMI) de-multiplexing, and cell barcode identification, generating cells × genes count matrix.

Quality control

Cell Ranger was used to calculate the single-cell expression matrix with the Seurat package (version 3.6.1) for cell filtration, normalization of data, reduction of dimensionality reduction, cell cluster, and differentially expressed gene analysis[28]. Cells with<300 genes or mitochondrial genes of>20 % were excluded for subsequent data analysis. DoubletFinder package (version 2.0.2) was used for calculating doublets [29]. The mean–variance-normalized bimodality coefficient (BCMVN) of each sample was used to calculate the neighborhood size (pK), and the number of artificial doublets (pN) was set to 0.25.

Clustering and cell-type identification

For each cell, the counts were logged normalized (1 + counts per 10,000). Variable genes were selected and projected into a low-dimensional subspace using canonical correlation analysis (CCA) among different samples for batch effects correction. A shared nearest neighbor graph was constructed based on the Euclidean distance in the low-dimensional subspace spanned by the selected significant principal components. Cells were visualized using a 2-dimensional *t*-distributed stochastic neighbor embedding (*t*-SNE) algorithm and Uniform Manifold Approximation and Projection for Dimension Reduction (UMAP) algorithm. Differential expression gene analysis was performed using the Wilcoxon rank-sum test. Cell types were allocated to each cluster using the abundance of known marker genes as described previously [30].

Differential genes expression analysis

Differential genes (DEGs) expression analysis of each cell type between young and old mice was conducted using the non-parametric two-sided Wilcoxon rank-sum test and only those with p adjust value < 0.1, |LogFC| > 10 % were considered to be aging-associated DEGs.

Gene Ontology (GO) enrichment analysis

Enrichr was used to perform gene set enrichment analysis against the Gene Ontology Biological Process 2018 version gene set collection. MSigDB Hallmark gene sets [31] were used to compute enrichment scores using Fisher's exact test. In both cases, we corrected multiple hypotheses testing using the Benjamini-Hochberg procedure. Results were shown by using the ggplot2 R package (https://ggplot2.tidyverse.org/) (version 3.2.1).

Transcriptional regulatory network analysis

Transcriptional regulatory network analysis was conducted using SCENIC (version 1.1.2.2) default parameters according to mm10 database of RcisTarget (version 1.6.0) [32]. For aging-associated transcriptional regulatory networks analysis, only aging-associated DEGs was used as inputs for inferring transcriptional regulators, and the findings were shown using the ggraph R package.

Cell-cell communication analysis

Cell-cell communication analysis was conducted utilizing the CellChat (version 1.1.0) [33]. Only the expression of ligands and receptors in above 10 percent of cells from either 'old' or 'young' groups were then analyzed, and only p value < 0.01 was retained for predicting cell–cell interaction. A p-value < 0.05 was regarded as significantly difference between young and aged mice.

Statistical analyses

All data were statistically analyzed using a two-tailed *t*-test to compare differences between 'old' and 'young' groups, assuming equal variance with the R package. P values were presented for bioinformatics analyses. A p value below 0.05 was considered to be statistically significant.

Results

Phenotypic characterization of testicular aging in mice

To characterize testicular aging, we firstly measured testis weight and body weight of male mice aged about 2 months (termed 'young' mice, n = 6) and aged 24 months (termed 'old' mice, n = 5) (Fig. 1A). As shown in Fig. 1B, 'old' mice showed a reduced ratio of testis weight to body weight compared with 'young' mice. Importantly, aged mice showed an increase in senescence-associated β-galactosidase (SA-β-Gal)-positive cells (Fig. 1C), indicating that aged testis shows a senescence phenotype. This result was further confirmed by the reduced Ki67- (Fig. 1D) and proliferating cell nuclear antigen (PCNA)-positive cells (Fig. 1E) in 'old' mice, suggesting increased cellular senescence in aged mice compared with that in 'young' mice, which is consistent with previous reports [34,35]. Taken together, these results indicate that aged testes display aging-associated injuries during physiological aging.

Construction of a single-cell transcriptomic atlas of mouse testis during aging

To determine the cellular and molecular changes in gene expression at single-cell resolution during mouse testicular aging, testicular tissues from three 'young' and three 'old' mice were used

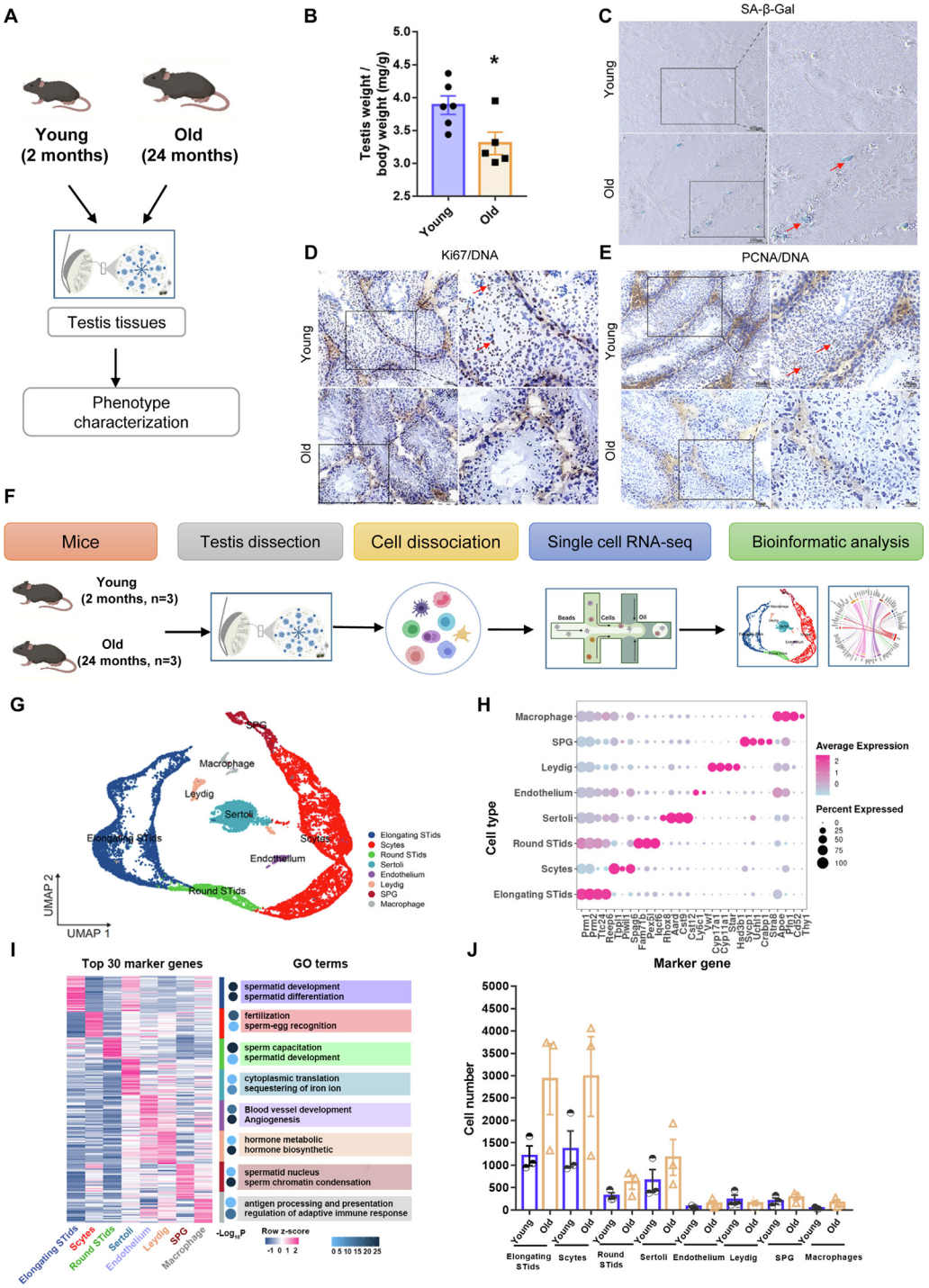

Fig. 1. Phenotypic characterization of testicular aging and construction of distinct cell types with transcriptional signature by ScRNA-Seq analysis of young and old mice testes. A. A schematic model of phenotypic analysis of testes of young (about 2 months, n = 6) and old mice (about 24 months, n = 5). **B.** Aged mice show reduced testis weight/body weight. **C**. Aged mice show increased senescence-associated beta-galactosidase (SA-β-Gal)-positive cells. **D**. Aged mice show reduced Ki67 (a marker of proliferating cells)-positive cells, a marker of aging. **E**. Aged mice show decreased proliferating cell nuclear antigen (PCNA)-positive cells, another marker of aging. **F**. Flowchart overview of the experimental design of this study. **G-H**. UMAP plot of cells from young and old mice testes tissues revealing 8 clusters of cell types (**G**) from a pool of 37,571 cells and canonical mark genes shown by dot plot (**H**). **I**. Heatmap showing top 30 marker genes in each cell types, and the relevant enriched GO terms. **J**. Bar plot showing cell numbers in each cell type of young and old mice.

for ScRNA-seq analysis as shown in the Flowchart (Fig. 1F). A pool of 37,571 cells was harvested for sequencing and subsequent downstream data analyses. A complex of these testicular cell types was unsupervised visualized using a uniform manifold approximation and projection (UMAP) algorithm, and eight-cell types were identified according to the expression of canonical cell-type-specific markers as reported previously [30]. These cell types were somatic cells including Leydig, Sertoli cells, macrophage cells, and endothelium cells, and germ cells including spermatogonia (SPG), spermatocytes (Scytes), round spermatids (round STids), and elongating spermatids (elongating STids) (Fig. 1G). We further mapped these cell types by comparing cell-type-specific marker genes and

relative pathways in the dot plots (Fig. 1H) and heatmaps (Fig. 1I). Gene Ontology (GO) analysis of the top 30 marker genes within each cell type demonstrated key characteristics that were correlated with their biological functions (Fig. 1I). Though there was a slight sample to sample variation, cell identity was largely preserved during aging, and aging dramatically increased the relative proportions of macrophage cells (Fig. 1J and Fig. S1A-B). Collectively, we generate a cellular roadmap of a single-cell transcriptome profiling of the mouse testis during aging.

Characterization of aging-induced alteration of molecular profiles in somatic cells

To understand the mechanisms underlying testicular aging, we investigated aging-induced changes in cellular and molecular events in somatic cells. We first discovered differentially expressed genes (DEGs) in four types of somatic cells including Sertoli, Leydig, macrophage, and endothelium cells during mouse testicular aging and revealed multiple shared and cell type-specific DEGs (507 DEGs for Sertoli cells, 170 DEGs for Leydig cells, 151 DEGs for endothelium cells, 158 DEGs for macrophage cells) in these somatic cells (Fig. 2A, and Fig. S2F). Notably, aged Leydig cells exhibited the greatest numbers of DEGs (Fig. 2A). GO analysis of these DEGs showed that aging-upregulated genes in multiple somatic cells were associated with 'protein homodimerization', 'positive regulation of cellular senescence', 'negative regulation of proteolysis', 'cellular response to oxidative stress', and 'cell cycle arrest' (Fig. 2B). These results were consistent with previous findings that aged testis exhibits increased oxidative stress [36,37] and apoptosis [38]. By contrast, GO analysis of shared DEGs showed that the top downregulated pathways among multiple somatic cell types were associated with 'response to wounding', 'receptor-mediated endocytosis', 'positive regulation of proteolysis', 'negative regulation of cell projection organization', and 'cellular hormone metabolic process' (Fig. 2C), indicating that aging compromises several key metabolic processes.

Further analysis showed that the overall gene set score [39] for 'steroid hormone-mediated signaling pathway' was reduced in aged mice, and this score was also reduced in Leydig and Sertoli cells but not in the endothelium cells (Fig. 2D-E). These results were consistent with previous findings that aging reduces testosterone production, and subsequently attenuates spermatogenesis [40]. We then examined the alterations of several key hallmarks of aging by analyzing the altercations of aging-associated gene sets in testes of 'young' and 'old' mice. Overall gene set score of 'ROS signaling' was increased in aged mice (Fig. 2F), which was consistent with previous reports in rodents [36,41]. Interestingly, Leydig and Sertoli cells showed particularly higher ROS signaling scores (Fig. 2G). This result was further confirmed by immunostaining results showing an increase in deoxyguanosine (8-OHdG), a marker of oxidative stress, in the testis sample of 'old' mouse (Fig. 2H). Because ROS is critical for intrinsic induction of apoptosis, we further examined elevated cleaved Caspase 3 in aged mice, a canonical marker for apoptosis (Fig. 2I). These results indicate that aged mice increases the production of ROS, which in turn may contribute to apoptosis, and comprise steroidogenesis.

We next dissected other hallmarks of aging. ScRNA-seq results showed that aged mice exhibited overall elevated gene set score for SASP genes (Fig. 2J), particularly, in Leydig, Sertoli, and endothelium cells (Fig. 2K). Notably, by annotating SASP-related DEGs in each cell type, we found that these three cell types showed both shared and heterogeneous differences that were increased in multiple SASP genes (Fig. 2L). We also found that aging augmented overall inflammatory-related gene set score, especially in Leydig, and Sertoli cells (Fig. 2M-**N**). Indeed, multiple inflammatory response-related genes were significantly increased in these three cell types (Fig. 2O), which was consistent with previous results showing that aging elevates inflammatory response [42,43]. Consistently, both shared and heterogeneous differences that were increased in multiple inflammatory genes were also found in the same cell types as in Fig. 2O. In addition, aging also reduced 'telomere maintenance via telomerase' (Fig. S2A-B) and 'DNA repair' (Fig. S2C-D) gene set scores, another two important hallmarks of aging. These results highlight critical roles of several hallmarks of aging such as increased SASP and inflammatory response, decreased telomere maintenance, and DNA repair in the testis during aging.

Because transcription factors (TFs) are critical for regulating gene expression, to better characterize aging-associated changes in transcriptomes, single-cell regulatory network inference and clustering (SCENIC) analysis [32] was performed to identify key TFs that may be associated with testicular aging. Our results showed that multiple shared or cell type-specific differentially changed TFs were blended into the network of aging-related DEGs in different somatic cells of the testis (Fig. 2P, and Fig. S2E). Notably, several TFs such as Klf6 and Jun6 in Sertoli cells and Leydig regulated a large amount of aging-associated DEGs. Interestingly, multiple increased nodal TFs including Nr2f6, Hes1, Jun6, and Etv5 were associated with inflammatory response and senescence during testicular aging. These TFs' changes may drive a hostile microenvironment via regulating aging-associated DEGs to induce the impairment of spermatogenesis during testicular aging.

Aging increases pro-inflammatory macrophages

Macrophages play a critical role in regulating inflammation and our ScRNA-seq results showed that aging induced the increase in the overall numbers of macrophages (Fig. 3A). This was further confirmed by immunostaining of macrophage markers in aged testes, which showed elevated levels of F4/80, CD68, and CD11b (Fig. 3B-D). Thus, we further characterized aging-induced alterations in molecular profiles of macrophages. By using marker genes, macrophages were clustered into 3 subtypes as reflected by UMAP plots (Fig. 3E-G, Fig. S3A), and interestingly, aging specifically increased subtype3 macrophages (Fig. 3E-F). GO terms of marker genes of these subtypes of macrophages showed that macrophage subtype1 was mainly involved in antigen processing and presentation (similar to classically activated M1 macrophage, pro-inflammatory), subtype2 macrophage was mainly involved in the regulation of endocytosis (similar to alternatively activated M2 macrophage, anti-inflammatory), and aging-specific subtype3 macrophage was mainly involved in the processes of mononuclear

Fig. 2. Cellular and molecular characteristics associated with aging in somatic cells. A. Venn diagram showing the distribution of differentially expressed genes (DEGs) (p adjust value < 0.05, |logFC| > 10 %) across each germ cell during mouse testicular aging.**B-C**. Representatives shared top GO terms of up-regulated (B) and down-regulated (C) genes in different germ cells during mouse testicular aging.**D.** Density plot revealing gene set score associated with 'steroid hormone-mediated signaling pathway' in mice testes of young and old mice. **E**. Violin plots showing decreased 'steroid hormone-mediated signaling pathway' gene set in Sertoli and Leydig cells of the aged mouse testis. **F**. Density plot revealing increased gene set scores for genes associated with 'ROS signaling' in young and old mice. **G**. Violin plots showing increased 'DNA repair' gene set in Sertoli and Leydig cells of aged mouse testis.**H**. Immunostaining showing increased 8-OHDG, a marker of oxidative stress, in aged mouse testis. **I**. Immunostaining showing increased cleaved caspase 3, a marker of apoptosis, in aged mouse testis. **J**. Density plot revealing gene set score of genes associated with 'SASP' in mice testes of young and old mice. **K**. Violin plots revealing increased 'SASP' gene set score in indicated cells of aged mouse testis.**L**. Network plot revealing DEGs genes associated with SASP in different somatic cells. **M**. Density plot revealing gene set score for genes associated with 'inflammatory response' in mice testes of young and old mice. **N**. Violin plots showing increased 'inflammatory response' gene set in indicated cells of aged mouse testis.**O**. Network plot revealing DEGs related to the inflammatory response in each somatic cells. **P**. Heatmap showing the differentially expressed TFs in different somatic cells during mouse testicular aging as shown by SCENIC analysis.

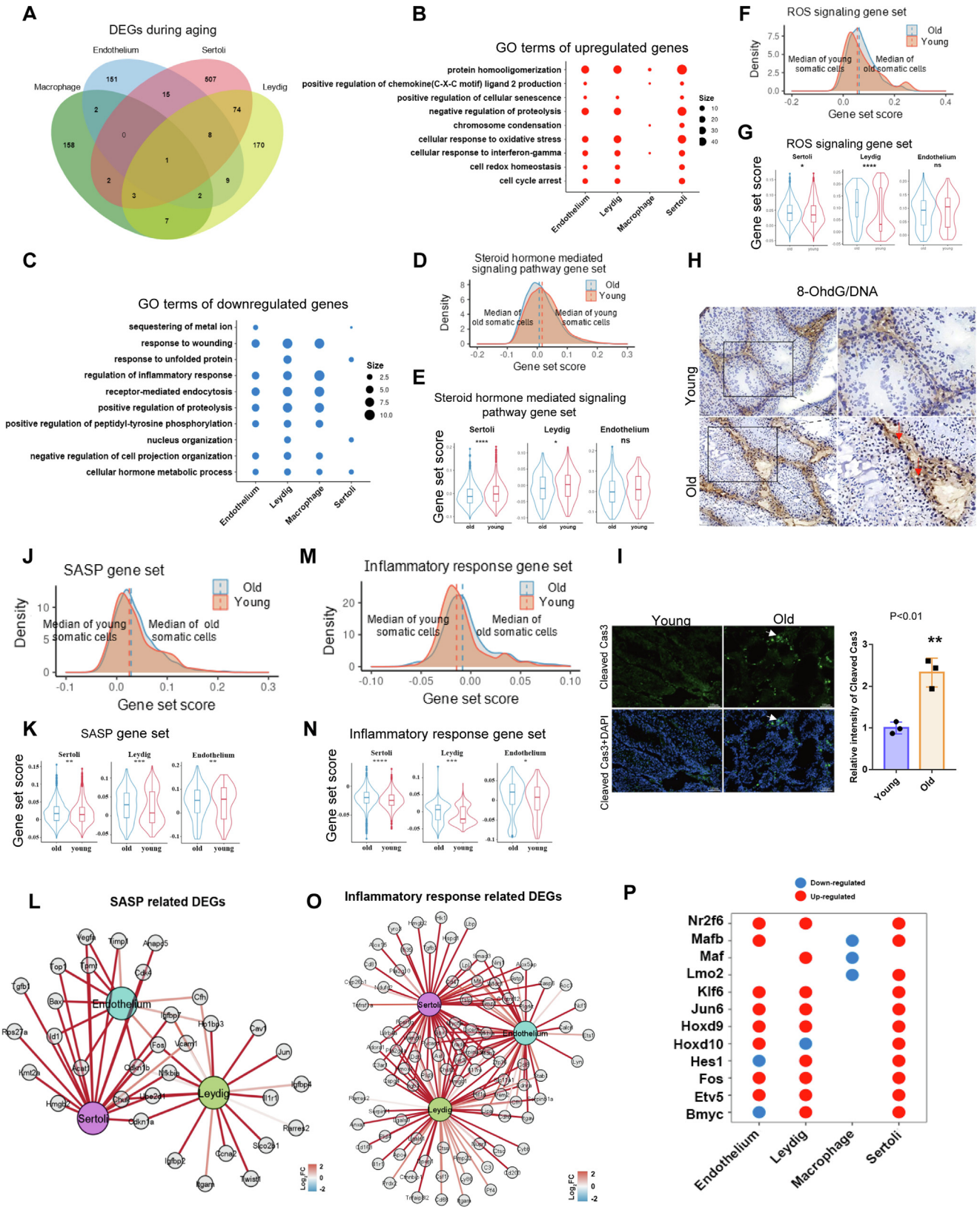
A
DEGs during aging
Endothelium
Sertoli
Macrophage
Leydig
151
507
15
2
74
0
8
158
170
1
2
9
3
2
7
B
GO terms of upregulated genes
protein homooligomerization
positive regulation of chemokine(C-X-C motif) ligand 2 production
positive regulation of cellular senescence
negative regulation of proteolysis
chromosome condensation
cellular response to oxidative stress
cellular response to interferon-gamma
cell redox homeostasis
cell cycle arrest
Endothelium
Leydig
Macrophage
Sertoli
Size
10
20
30
40
C
GO terms of downregulated genes
sequestering of metal ion
response to wounding
response to unfolded protein
regulation of inflammatory response
receptor-mediated endocytosis
positive regulation of proteolysis
positive regulation of peptidyl-tyrosine phosphorylation
nucleus organization
negative regulation of cell projection organization
cellular hormone metabolic process
Endothelium
Leydig
Macrophage
Sertoli
Size
2.5
5.0
7.5
10.0
D
Steroid hormone mediated signaling pathway gene set
Old
Young
Median of old somatic cells
Median of young somatic cells
Density
Gene set score
E
Steroid hormone mediated signaling pathway gene set
Sertoli
Leydig
Endothelium
****
*
ns
Gene set score
old
young
F
ROS signaling gene set
Old
Young
Median of young somatic cells
Median of old somatic cells
Density
Gene set score
G
ROS signaling gene set
Sertoli
Leydig
Endothelium
*
****
ns
Gene set score
H
8-OhdG/DNA
Young
Old
I
Young
Old
Cleaved Cas3
Cleaved Cas3+DAPI
P<0.01
**
Relative intensity of Cleaved Cas3
Young
Old
J
SASP gene set
Old
Young
Median of young somatic cells
Median of old somatic cells
Density
Gene set score
K
SASP gene set
Sertoli
Leydig
Endothelium
Gene set score
old
young
L
SASP related DEGs
Endothelium
Leydig
Sertoli
M
Inflammatory response gene set
Old
Young
Median of young somatic cells
Median of old somatic cells
Density
Gene set score
N
Inflammatory response gene set
Sertoli
Leydig
Endothelium
Gene set score
old
young
O
Inflammatory response related DEGs
Sertoli
Endothelium
Leydig
Log2FC
P
Down-regulated
Up-regulated
Nr2f6
Mafb
Maf
Lmo2
Klf6
Jun6
Hoxd9
Hoxd10
Hes1
Fos
Etv5
Bmyc
Endothelium
Leydig
Macrophage
Sertoli

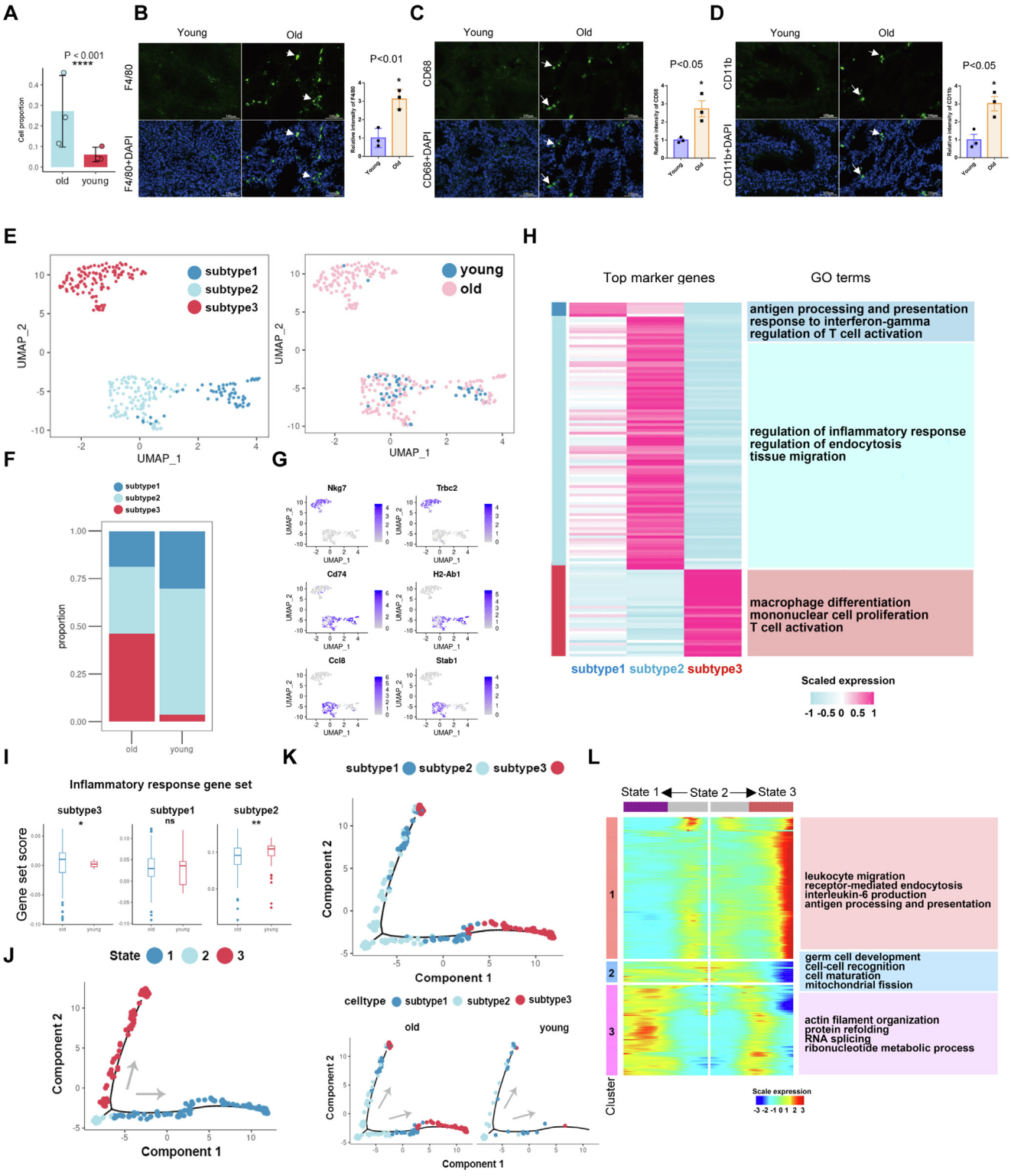

Fig. 3. Cellular and molecular characteristics associated with aging in macrophages. A. Bar plot showing increased overall macrophages in aged mice. **B-D**. Immunostaining showing increased macrophage markers F4/80, CD68, and CD11b in aged mice. **E-F**.UMAP (E) and bar plot (F) showing the distribution of three types of macrophages in mouse testis. **G**. Representative marker genes of indicated macrophage subtypes. **H**. Heatmap showing GO terms of top marker genes in each macrophage subtypes, and with unique functions.**I**. Bar plot showing increased 'inflammatory response gene set' score in aging-specific subtype3 macrophages. **J-K.** Pseudotime analysis of macrophages in the mouse testis. Cells were colored by 3 cell states (**J**) and different subtypes (**K**). The arrows indicate the directions of differentiation trajectories. **L**. Heatmap showing the expression profiles of 3 clusters at two branches (state 2 to state 1, and state 2 to state 3) along the pseudotime based on top aging-associated DEGs in macrophage subtypes. Representative enriched GO terms of the corresponding 3 clusters were listed on the right.

cell proliferation, and T cell activation (Fig. 3H). Interestingly, subtype3 macrophages showed increased gene set scores of 'inflammatory response gene set' (Fig. 3I), highlighting the critical roles of this type of aging-specific macrophage in mediating testicular inflammation. We further characterized aging-induced DEGs and related pathways in macrophage cells. GO analysis showed that

aging-associated upregulated DEGs were enriched in pathways related to multiple processes in inflammatory response such as 'type I interferon secretion', in subtype1 macrophages and 'Toll-like receptor 4 signaling pathway' in subtype2 macrophages (**Fig. S3**).

Distinct subtypes of macrophages can be switched to each other in response to a variety of stimuli [44]. To further explore how aging may affect macrophage phenotypes switch, we constructed the lineage trajectory of macrophages and revealed two branches of three states (State 2 to state 1, and state 2 to state 3) of macrophages along the pseudotime trajectory (Fig. 3J-K), and found that subtype3 macrophages were mainly distributed in state 3. Branched expression analysis modeling (BEAM) [45] showed three clusters, and relative GO pathways in each cluster were included (Fig. 3L). For instance, GO analysis indicated that Cluster 1 showed dramatically increased defined genes along the trajectories, and signature genes were mainly enriched in pathways related to 'leukocyte migration', 'receptor-mediated endocytosis', 'interleukin-6 production' and 'antigen processing and presentation'. Cluster 3 was mainly enriched in pathways associated with 'actin filament organization', 'RNA splicing', and 'ribonucleotide metabolic process' (Fig. 3L). Collectively, our results demonstrate that subtype3 macrophage cells are specially hyperactivated in aged testis. Overall, the increased macrophages, especially proinflammatory subtype3 macrophages, that are induced in aged cells, may constitute a major contribution to the hostile inflammatory microenvironment in testicular aging.

Characterization of the aging-associated cellular and molecular profiles of germ cells in mouse testis

Spermatogenesis is a conserved complex program that is driven by interactions of multiple germ cells and somatic cells. To dissect how aging affects cellular and molecular profiles of germ cells in mouse testis, we then generated a UMAP algorithm of germ cells, and identified four subtypes of germ cells including SPG, Scytes, round STids, and elongating STids (Fig. 4A). Based on this map, we identified aging-associated transcriptional changes in individual germ cells. A total of 722 DEGs genes in germ cells (p value < 0.05) were identified, and aged SPG exhibited the greatest numbers of differentially expressed genes compared with that of 'young' mice. Multiple cell type-specific and shared DEGs were also discovered (Fig. 4B, and Fig. S2F), GO analysis of these DEGs showed that top upregulated pathways among multiple germ cells were associated with 'regulation of inflammatory response', 'reactive oxygen species metabolic process', and 'G1 DNA damage checkpoint', and 'cellular response to metal ion' (Fig. 4C). Top downregulated pathways in multiple germ cells were related to 'response to wounding', 'response to oxidative stress', 'regeneration', 'regulation of cellular amine metabolic process', and 'cellular response to nutrient levels' (Fig. 4D). These results indicate that multiple processes such as increased oxidative stress and decreased energy metabolism and regeneration in germ cells may be involved in testicular aging.

Further analysis showed that the 'DNA repair' gene set scores were reduced in multiple germ cells (Fig. 4E-F), and this result was further supported by immunostaining results showing increased phoshorylated γ-H2A.X, a marker of DNA damage and DNA double-strand breaks [46] in aged mice compared with that in 'young' mice (Fig. 4G). Additionally, 'regeneration'-associated genes were significantly decreased in four germ cell types of 'old' mice (Fig. 4H), and especially in round STids, and elongated STids (Fig. 4I). We also annotated each DEGs in different germ cells associated with 'DNA repair' and 'regeneration' (Fig. S4A-B). The impairment of DNA repair system is associated with premature aging [47], and effective DNA repair is required for the normal male germ system to produce spermatozoa during a long lifetime [47]. The compromised 'DNA repair' in germ cells, as well in somatic cells may be involved in aging-associated subfertility. Because regenerative ability is essential for producing mature germ cells, its downregulation (Fig. 4F) further supported the notion of compromised spermatogenesis during aging. Consistent with the findings in somatic cells, gene set score for 'telomere maintenance via telomerase gene set', another hallmark of aging was significantly decreased in Scytes, round STids, and elongating STids in aged mice (Fig. 4J-K). Gene set score of 'steroid hormone mediated signaling pathway' was also significantly decreased, especially in Scytes, round STids, and elongating STids in aged mice (Fig. S4C-D). These results were in line with the results in Leydig and Sertoli cells, and these changes possibly contributed to the reduced number and quality of sperm in aged mice. Aging also increased gene set score for 'ROS signaling gene set', another hallmark of aging, in certain germ cells (Fig. S4E-F). It is possible that this increased ROS is associated with elevated SASP, increased inflammation, compromised DNA repair, which constitutes a major hostile testicular niche that may consequently promote testicular aging.

Next, SCENIC analysis was performed and revealed that multiple shared or cell-type-specific TFs were incorporated into a network of aging-related DEGs in different germ cells of the testis (Fig. 4L-M). Notably, the majority of the increased nodal TFs were associated with inflammatory responses during testicular aging. These TFs include Spi1, Hes1, Junb, hmgb3, Etv5, and hmgb2 (Fig. 4L-**M**). These results indicate a potentially critical role of these TFs in mediating inflammatory responses in testicular aging.

Characterization of the unique gene-expression signatures of germ cells at stepwised and sequential developmental stages during testicular aging

To determine the gene-expression dynamics of spermiogenesis during which mature sperms are produced from SPG, during aging, unsupervised analysis of germ cells DEGs was performed, and four subtypes of germ cells (Cluster 1 to Cluster 4) were discovered. Principal component analysis (PCA) showed that four germ cell clusters including SPG, Scytes, round STids, and elongated STids were sequentially and step-wisely developed as shown by pseudotime analysis (Fig. 5A-B). Aging did not obviously affect the distribution of these cells along the trajectories (Fig. 5A), which may be due to the declined but still functional ability of the testes to produce sperms in aged mice. Among these four clusters, GO terms of their cell-type-specific genes showed relatively enriched pathways along the pseudotime (Fig. 5B). For example, cluster 1 showed dramatically decreased defined genes along the trajectories, and signature genes were enriched for pathways associated with

Fig. 4. Cellular and molecular characteristics associated with aging in germ cells. A. UMAP showing different germ cell types in young and old mice testes tissues. **B**. Venn diagram showing the distribution of DEGs across each germ cell during mouse testicular aging. **C-D**. Representatives shared top GO terms of aging-associated upregulated (**C**) and downregulated (**D**) genes in different germ cells during mouse testicular aging.**E.** Density plot revealing gene set score of genes associated with 'DNA repair' in germ cells of mice testes of young and old mice. **F**. Violin plots showing decreased 'DNA repair' gene set scores in different germ cells of aged mouse testis. **G**. Immunostaining revealing an increase in phoshorylated γ-H2AX, a marker for DNA damage, in aged mice. **H.** Density plot showing gene set scores of genes associated with 'regeneration' in germ cells of mice testes of young and old mice. **I**. Violin plots showing decreased ''regeneration' gene set score in indicated cell types of aged mouse testis. **J**. Density plot revealing gene set score of genes associated with 'telomere maintenance via telomerase gene set' in germ cells of mice testes of young and old mice. **K**. Violin plots showing decreased 'telomere maintenance via telomerase gene set' gene set score in different germ cells of aged mouse testis. **L-M**. Heatmap showing the differentially expressed TFs (**L**) and their DEGs (**M**) in germ cells during mouse testicular aging as shown by SCENIC analysis.

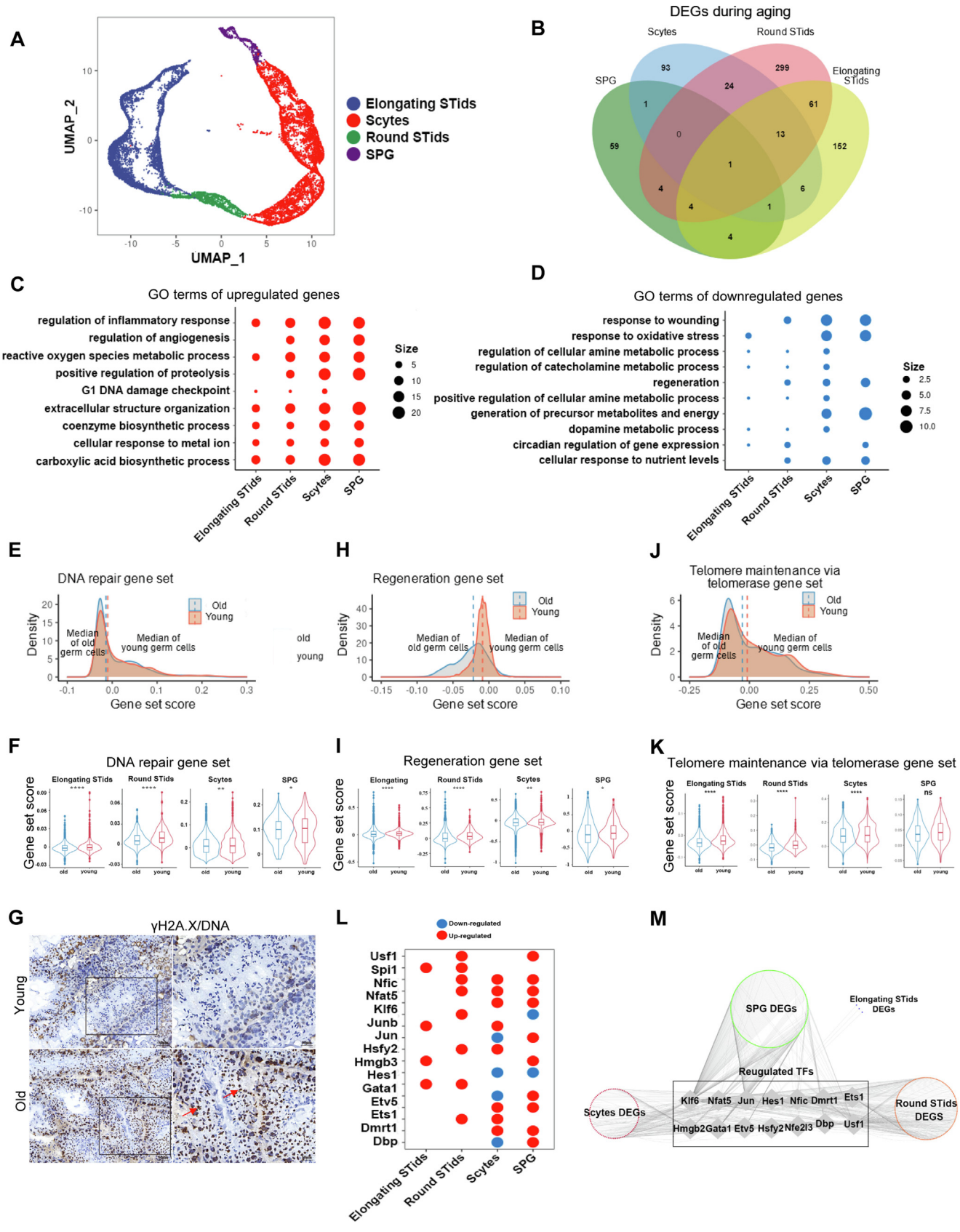
A
UMAP_2
UMAP_1
Elongating STids
Scytes
Round STids
SPG
B
DEGs during aging
Scytes
Round STids
SPG
Elongating STids
93
299
24
1
61
0
13
59
152
1
4
6
4
1
4
C
GO terms of upregulated genes
regulation of inflammatory response
regulation of angiogenesis
reactive oxygen species metabolic process
positive regulation of proteolysis
G1 DNA damage checkpoint
extracellular structure organization
coenzyme biosynthetic process
cellular response to metal ion
carboxylic acid biosynthetic process
Size
5
10
15
20
Elongating STids
Round STids
Scytes
SPG
D
GO terms of downregulated genes
response to wounding
response to oxidative stress
regulation of cellular amine metabolic process
regulation of catecholamine metabolic process
regeneration
positive regulation of cellular amine metabolic process
generation of precursor metabolites and energy
dopamine metabolic process
circadian regulation of gene expression
cellular response to nutrient levels
Size
2.5
5.0
7.5
10.0
Elongating STids
Round STids
Scytes
SPG
E
DNA repair gene set
Density
Old
Young
Median of old germ cells
Median of young germ cells
old
young
Gene set score
H
Regeneration gene set
Density
Old
Young
Median of old germ cells
Median of young germ cells
Gene set score
J
Telomere maintenance via telomerase gene set
Density
Old
Young
Median of old germ cells
Median of young germ cells
Gene set score
F
DNA repair gene set
Gene set score
Elongating STids
Round STids
Scytes
SPG
old
young
I
Regeneration gene set
Gene set score
Elongating
Round STids
Scytes
SPG
old
young
K
Telomere maintenance via telomerase gene set
Gene set score
Elongating STids
Round STids
Scytes
SPG
ns
old
young
G
γH2A.X/DNA
Young
Old
L
Down-regulated
Up-regulated
Usf1
Spi1
Nfic
Nfat5
Klf6
Junb
Jun
Hsfy2
Hmgb3
Hes1
Gata1
Etv5
Ets1
Dmrt1
Dbp
Elongating STids
Round STids
Scytes
SPG
M
SPG DEGs
Elongating STids DEGs
Reugulated TFs
Klf6 Nfat5 Jun Hes1 Nfic Dmrt1 Ets1
Hmgb2 Gata1 Etv5 Hsfy2 Nfe2l3 Dbp Usf1
Scytes DEGs
Round STids DEGS

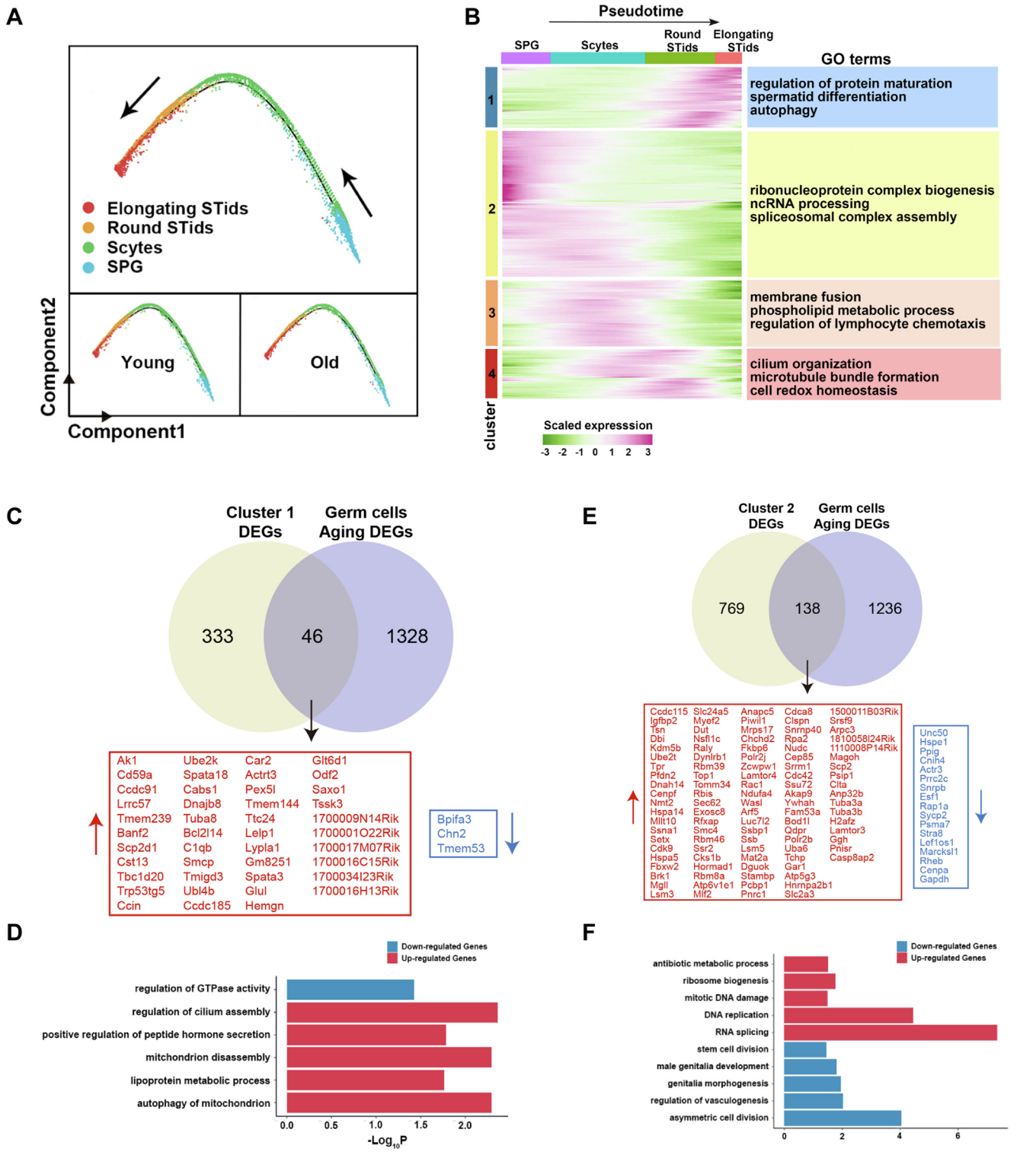

Fig. 5. Aging-associated cellular and molecular changes along the trajectories of germ cell differentiation. A. Pseudotime trajectory of germ cells differentiation analyzed by Monocle in young and old testes. The arrow points to the development direction of spermatogonia.**B**. Heatmap revealing the gene expression profiles of 4 clusters along the differentiation trajectory from SPG to elongating STids based on top aging-associated DEGs in germ cells. Represented enriched pathways of the relevant 4 clusters were shown on the right. **C**. Violin plot revealing shared genes between cluster 1 DEGs and aging-associated DEGs of germ cells. **D**. Bar plot revealing enriched pathways of shared genes listed in **C**. **E**. Violin plot revealing shared genes between cluster 2 DEGs and aging-associated DEGs of germ cells. **F**. Bar plot revealing enriched pathways of shared genes listed in **E**.

'regulation of protein maturation', 'spermatid differentiation', and 'autophagy' (Fig. 5B). Cluster 2 showed defined genes enriched in 'ribonucleoprotein complex biogenesis', 'ncRNA processing', and 'spliceosomes complex assembly'. Cluster 3 showed genes dramatically increased along the trajectories. Go analysis showed that the enriched pathways of these genes were for 'membrane fusion',

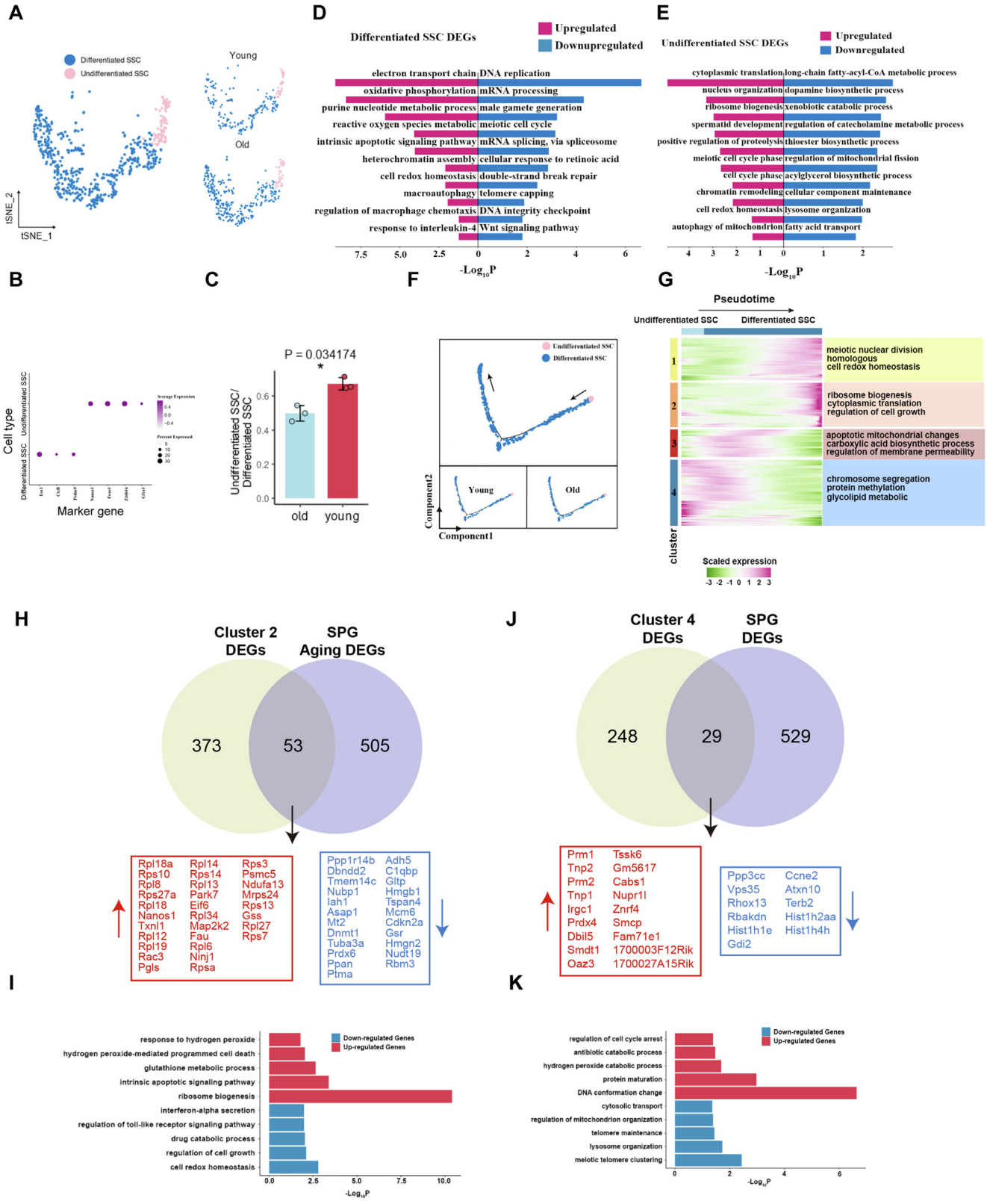

Fig. 6. Aging-associated cellular and molecular changes in SPG. A. *t*-SNE showing the distribution of undifferentiated SSCs and differentiated SSCs in young and old group of mice testes. **B**. Dot plots showing representative marker genes of undifferentiated SSCs and differentiated SSCs.**C**. The ratio of undifferentiated SSCs to differentiated SSCs in young and old mice testes. **D-E**. Diagram showing the enrichment of GO terms of aging-associated upregulated and downregulated DEGs in differentiated SSCs (**D**) and undifferentiated SSCs (**E**).**F**. Pseudotime analysis of undifferentiated SSCs to differentiated SSCs in the mouse testis. Different cell types were shown in relevant colors. The arrows indicates the directions of differentiation trajectories from undifferentiated SSCs to differentiated SSCs. **G**. Heatmap revealing the expression characteristic of 4 clusters among the pseudotime of undifferentiated SSCs to differentiated SSCs based on top aging-associated DEGs in SPGs. Representive enriched pathways of the relevant 4 clusters were listed on the right.**H**. Violin plot revealing shared genes between cluster 2 DEGs and aging-associated DEGs of SPG in mouse testis. **I**. Bar plot revealing enriched upregulated and downregulated pathways of shared genes showed in **H**.**J**. Violin plot revealing shared genes between cluster 4 DEGs and aging-associated DEGs of SPG. **K**. Bar plot revealing enriched upregulated and downregulated pathways of shared genes shown in **J**.

'phospholipid metabolic process' and 'regulation of lymphocyte chemotaxis'. These results highlight the critical roles of these signaling pathways in germ cells development.

To explore age-associated changes along the trajectories during germ cells differentiation, we identified four cluster-specific DEGs between 'old' and 'young' groups and subsequently compared these DEGs with age-related DEGs. Our results showed that multiple cluster-specific DEGs were overlapped with aging-related DEGs from cluster 1 to cluster 4 (Fig. 5C-F**,** Fig. S5G, H). Among 46 genes shared between cluster 1-specific DEGs and age-related DEG, GO analysis showed that the upregulated genes were enriched in pathways associated with 'mitochondrial disassembly', and 'lipoprotein metabolic process', and the downregulated genes were associated with 'regulation of GTPase activity' (Fig. 5C-D). GO analysis among 138 DEGs overlapped between cluster 2-specific DEGs and germ cells age-associated DEGs revealed that the upregulated genes were enriched in 'RNA splicing', 'DNA replication', and 'mitochondrial DNA repair' (Fig. 5E-F). These results show the dysregulation of several steps along with the germ cell differentiation, especially for the early stage of germ cell differentiation, reflecting critical changes in the aged testes, which likely contribute to mouse testicular aging.

Aging disrupts the balance between undifferentiated SSCs and differentiated SSCs

The balance between self-renewal of SPG and the differentiation of SPG into mature spermatids is critical for steady-state spermatogenesis. As SPG is critical for aging-associated spermatogenesis, we further explored aging-associated SPG by analyzing our ScRNA-seq data. We divided SPG into undifferentiated spermatogonial stem cells (SSCs) and differentiated SSCs (Fig. 6A-B) based on the expression of several marker genes as described previously [16]. We also mapped top expression genes in undifferentiated SSCs and differentiated SSCs. Consistent with previous results, undifferentiated SSCs only expressed spermatogonial stem cell marker genes (e.g., Kit, Stra8, Dmrts, and Sohlhs), but they did not express differentiation marker genes (Fig. S5A). The differentiation of undifferentiated spermatogonia to differentiated spermatogonia is critical for spermatogenesis [48]. Notably, aging dramatically reduced the ratio of undifferentiated SSCs to differentiated SSCs (Fig. 6C), indicating that aging disrupts the balance between stem cell maintenance and stem cell differentiation, and these changes may finally trigger aging-associated stem cell exhaustion.

To characterize aging-associated alterations in SPG, we further discovered 146 DEGs in undifferentiated SSCs and 441 DEGs in differentiated SSCs (Fig. S5B-C). GO analysis of these DEGs revealed that aging-upregulated top pathways in differentiated SSCs were related to 'electron transport', 'oxidative phosphorylation', 'purine nucleotide metabolic process', 'reactive oxygen signaling pathways' and 'intrinsic apoptosis pathway' (Fig. 6D). By contrast, aging-downregulated top pathways in differentiated SSCs were related to 'DNA replication', 'mRNA processing', 'male gamete generate', 'meiotic cell cycles', 'mRNA splicing', 'cellular response to retinoic acid', and 'double-strand break repair' (Fig. 6D). These results indicate that aging may affect multiple processes such as disrupted mitochondrial functions, and inhibited DNA replication and DNA repair in differentiated SSCs. In undifferentiated SSCs, GO analysis showed that aging-induced top upregulated pathways were related to 'cytoplasmic translocation', 'nucleus organization', 'ribosome biogenesis', 'positive regulation of proteolysis' (Fig. 6E). By contrast, aging-induced top-downregulated pathways were associated with 'long-chain fatty-acid-CoA metabolic process', 'xenobiotic catabolic process', 'regulation of mitochondrial fission', 'lysosome organization' and others (Fig. 6E). These results demonstrate that aging may compromise multiple metabolic processes in undifferentiated SSCs. Collectively, these results highlight the critical roles of these pathways in SPG that may be involved in testicular aging.

We next sought to further explore the molecular events in SPG during mouse testicular aging, we mapped the differentiation trajectories of undifferentiated SSCs to differentiated SSCs by pseudotime analysis as reflected by the sequential and stepwise developmental process. Aging did not dramatically affect the distribution of cell types along the trajectories (Fig. 6F**).** To explore the gene-expression dynamics during the process from undifferentiated SSCs to differentiated SSCs, unsupervised analysis of DEGs in SPG was performed and four subtypes (cluster 1 to cluster 4) (Fig. 6G) were discovered with respect to the pseudotime. GO analysis showed that each cluster expressed different GO terms. For instance, cluster 1 defined genes were dramatically decreased in undifferentiated SSCs with the trajectories, which were enriched with pathways associated with 'meiotic nuclear division', and 'homologous'. By contrast, cluster 4 defined genes were progressively increased, which were enriched with pathways related to 'chromosome segregation', and 'protein methylation' (Fig. 6G**).** These results highlight the critical roles of these pathways in the transition of undifferentiated SSCs to differentiated SSCs.

We further determined age-associated changes along the trajectories in the transition process from undifferentiated SSCs to differentiated SSCs. By analysis of overlapped genes between age-associated DEGs and four cluster-specific DEGs, we revealed that multiple cluster-specific genes were overlapped with aging-related DEGs. For instance, the 125 genes overlapped between Cluster 1-specific DEGs and age-related DEGs (Fig. S5D**)** were enriched in pathways associated with 'meiosis I cell cycle process', 'protein targeting', and 'mitochondrial organization' (Fig. S5E**).** GO analysis of the 53 shared genes between Cluster 2-specific genes and age-related DEGs revealed that the top 30 upregulated genes were mainly enriched in 'ribosome biogenesis', and 'intrinsic apoptotic signaling pathway', while the top 23 downregulated genes were enriched in 'cell redox homeostasis' and 'regulation of cell growth' (Fig. 6H**-I**). 28 genes were shared between cluster 3-specific DEGs and age-associated DEGs (Fig. S5F), and the upregulated genes were enriched in 'mitochondrial organization' and 'heterochromatin assembly' (Fig. S5G**).** GO analysis of the 29 shared DEGs between cluster 4-specific genes and age-associated DEGs revealed that the up-regulated genes were mainly associated with 'DNA conformation change' and 'protein maturation', and the downregulated genes were mainly associated with 'meiotic telomere clustering' and 'lysosome organization' (Fig. 6J**-K).** Taken together, these results suggest that aging-associated changes of key pathways are involved in the transition of undifferentiated SSCs to differentiated SSCs during testicular aging, which finally disrupts the balance between undifferentiated SSCs and differentiated SSCs.

Aging induces alterations in intercellular communications

Characterization of ligand-receptor pairs offers important information for understanding central cellular components that affect tissue fate. To understand the potential interactions of ligand-receptor between somatic cells and germ cells during mouse testicular aging, we determined the changes of receptors and ligands interaction by CellChat analysis [49]. We first examined cell–cell interaction numbers among different somatic cells and germ cells in 'old' and 'young' mice. Though the numbers of interactions among different cell types varied, aging reduced the number of inferred interactions, while it increased the interaction weight/strength among different cell types (Fig. 7A-B). Moreover, the differential number of interactions (Fig. 7C**,** Fig. S6A-B) and differential interaction strengths (Fig. 7D**,** Fig. S6C-D) between 'old' and 'young' mice analysis revealed dominant changes in macrophages. These results indicate that aging induces the intercellular interactions in niche cells, which may contribute to testicular aging. We

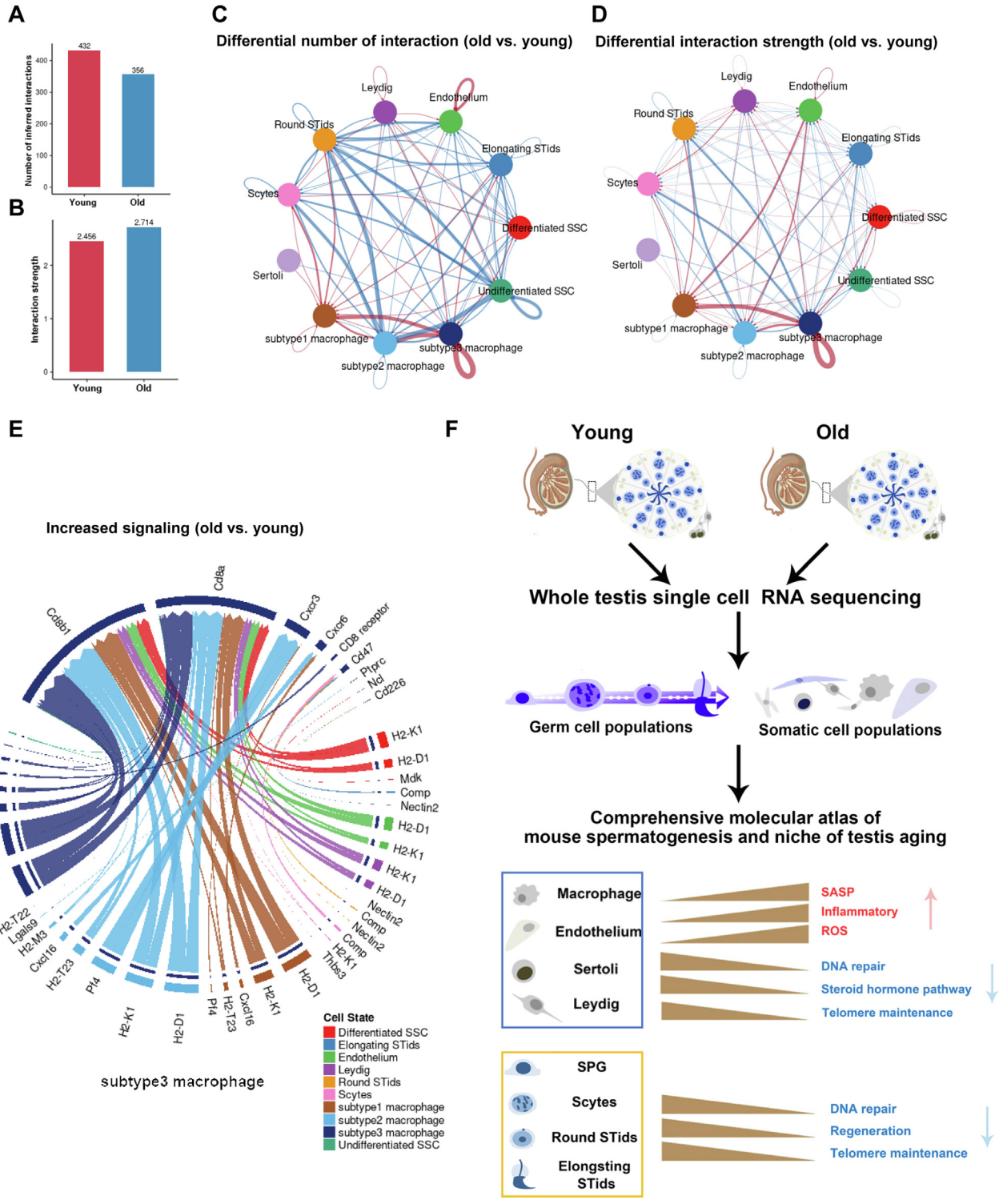

Fig. 7. Aging-associated alterations of cell–cell interactions.A-B. Bar plots showing interaction numbers (**A**) and strengths (**B**) in young and old mice testes.**C-D**. Chordal graph (by CellChat analysis) of differential interaction numbers (**C**) and interaction strength (**D**) of each cell type of mice testes between old and young mice, the thickness degree indicates the interaction numbers or interaction strength between sender and receiver cells.**E**. Chordal graph of increased ligand-receptor pair in aging-specific macrophages. The edge width represents the communication probability. **F**. A schematic model of the ScRNA-seq profiles revealing aging-associated cellular and molecular microenvironment features in mouse testis.

next determined the specific ligand-receptor pairs using the previous established database [50] and examined those ligand and receptor expression levels in both 'old' and 'young' mice. Our results discovered multiple increased ligand-receptor pairs in aging-specific macrophages (subtype3 macrophage) (Fig. 7E). For instance, aging increased receptor/ligand pairs such as H2-K1/CD8b1, H2-K1/CD8a, H2-D1/Cd8b1, H2-D1/CD8a between subtype1, subtype2 macrophages, multiple somatic cells, and aging specific macrophages (subtype3 macrophage). These results may indicate an increase in the proinflammatory microenvironment because H2-K1 (histocompatibility 2, K1, K region), H2-D1 (histocompatibility 2, D region locus 1), Cd8a (CD8 antigen, alpha chain),

and Cd8b (CD8 antigen, beta chain) play critical roles in antigen-presentation and/or cytotoxic T cell-antigen interactions [51]. Altogether, these findings signify the changes in receptor/ligand interactions in aged testes of mice, especially in aging-specific macrophages, which may promote the proinflammatory microenvironment and contribute to testicular aging.

Discussion

In this study, we construct the first comprehensive ScRNA-seq atlas of mouse testicular aging, and delineate aging-associated cell-type-specific molecular changes in the mice testes, highlighting not only several critical processes but also heterogenicity of different cell types during testicular aging (Fig. 7F). Specifically, we provided gene-expression signatures of germ cells and somatic cells in the mouse testis during aging. Aging-related DEG analysis demonstrated that multiple biological processes such as compromised 'DNA repair', 'regenerative', 'telomere maintenance' were major aging-associated features in germ cells, and increased 'SASP', 'ROS' and ''inflammation" were major aging-associated characteristics in somatic cells. Moreover, disrupted balance between undifferentiated SSCs and differentiated SSCs cells was another major feature of aging. Interestingly, the most important finding was that aging increased macrophages numbers, especially for a subtype of aging-specific pro-inflammatory macrophages, which was likely to contribute to the aging-associated hostile inflammatory microenvironment in the testis. Taken together, our results provide enormous resources for better understanding of the molecular mechanisms of testicular aging, which may shed light on developing novel therapeutic interventions against age-associated subfertility.

Somatic cells are known for their supporting roles in producing mature germs. Of those, Sertoli cell is a kind of structural supporting cell and it also provides nutrients, and Leydig cell is mainly responsible for producing testosterone to support spermatogenesis. Here, ScRNA-seq results not only highlighted several critical processes but also revealed heterogeneity of different cell types during testicular aging. For instance, though previous studies revealed age-associated increase of oxidative stress in the testis [41], our ScRNA-seq results showed that the increased gene set score for 'ROS signaling' was mainly restricted to somatic cells, and to a lesser extent in germ cells. These results demonstrated cell-type-specific changes in certain aging hallmarks of testicular aging. The increased ROS signaling may contribute to other hostile events such as aging-associated elevation of inflammation and SASP, increased apoptosis, and inhibited steroidogenesis in somatic cells as revealed by our ScRNA-seq results, which then may impair spermatogenesis from germ cells in aged testes. Furthermore, increased oxidative stress and/or comprised antioxidant systems have been observed in multiple aging-associated contexts [52,53]. These results also suggest that oxidative stress may serve as one of the biomarkers for testicular aging and a potential diagnosing and/or therapeutic target for aging-associated male fertility preservation.

Furthermore, we revealed that disrupted the balance betweeen undifferentiated SSCs and differentiated SSCs cells was another major feature of aging. SPG is indispensable for producing mature sperms and for male fertility. Previous studies have shown that aging compromises stem cell regeneration ability [54,55], and SSCs undergo age-associated epigenetics and functions alterations [56]. Here, though overall SPG proportions were largely preserved during testicular aging, our in-depth analysis revealed that aging decreased the ratio of undifferentiated SSCs to differentiated SSCs, suggesting that aging induces a loss of quiescent undifferentiated stem cell populations, which may result in reduced spermatogenic efficiency and subsequent stem cell exhaustion, as well as the gradually declined fertility in aged men [57,58]. Accordingly, pseudotime trajectories analysis revealed several key molecular profiles associated with the progression of undifferentiated SSCs to differentiated SSCs, and multiple aging-associated DEGs were critical in these processes (Fig. 6J-**K**). Notably, aging regulated multiple biological processes such as downregulation of 'long-chain fatty-acyl-CoA metabolic process', and 'fatty acid transport' in undifferentiated SSCs, and elevation of 'purine nucleotide metabolic process' in differentiated SSCs, highlighting critical roles of the metabolic process during testicular stem cell aging (Fig. 6E). Overall, these results provide novel mechanisms involved in the maintenance of undifferentiated SSCs and differentiated SSCs during testicular aging, which may play a critical role in aging-associated decline in spermatogenic efficiency.

Aging has been linked to profound changes in immune systems by affecting multiple immune cells including macrophages [59]. Previous studies mainly focused on the characterization of morphology changes in macrophage during testicular aging [42,60]. However, how aging affects the molecular characteristics of macrophages is largely unclear. Interestingly and importantly, we found that aging induced the increase in the numbers of macrophage cells, especially for the subtype of aging-specific pro-inflammatory macrophages (positive for Nkg7 and Trbc2), which likely contributed to the aging-associated hostile proinflammatory microenvironment in testis and subfertility of aged mice. These results highlight the potential roles of aging-associated macrophages in testicular aging. Future studies aiming at further characterization of their roles in testicular aging is an interesting topic.

Interesitngly, our results showed that multiple testes aging DEGs were overlapped with the global aging genes identified previously [24] (Fig. S1C), and aging DEGs in testes also showed similar trend for upregulation or downregulation as reported previously in other tissues or cells [19,61,62] (Fig. S1E). We also identified multiple testes macrophage-specific aging-associated genes compared with the previously identified macrophage aging genes in other tissues [24] (Fig. S1D), indicating that testes macropahges may exhibit unqiue functions.

Overall, we showed that senescence, and inflammation [39,63] may serve as potential signaling markers and even therapeutic targets for testicular aging. Interestingly, senescence is also a key charactersitc of ovary aging [64]. Future studies to compare the difference and common pathways between male and female aging is also an interesting topic. Notably, this study mainly focused on comparing aged mice with young mice, and future studies including more time points throughout the life cycle of mice (e.g., middle age) may provide more information for in-depth understanding of testicular aging. In addition, since reduced sexual activity is also an aging-associated characteristic, here, we used model mice housed with the same gender, and thus our results may be different from aged mice housed in mixed-gender. Future studies using aged mice in mix-gender may provide more information for understanding of testicular aging. Interestingly, several pathways such as cellular senescence, apoptosis, DNA damage, and compromised stem cell maintenance that have been identified in our studies were also involved in switch from non-aging asexual reproduction to aging and sexual reproduction [65], highliting the crtical role of these pathways in testicular aging.

Conclusion

In conclusion, to our knowledge, this study provides the first comprehensive single-cell transcriptomic landscape of mouse testicular aging and expands the understanding of cell-type-specific gene profiles of mouse testis during aging. Importantly, the ScRNA-seq results can serve as an enormous resource and platform for the future dissection of aging-associated subfertility. Moreover, this study could open potential new avenues such as targeting oxidative stress and inflammation for developing diagnostic or targeted therapeutics to protect against physiological testicular aging

and/or for assisting reproductive therapies for male fertility preservation.

Ethics statements

All experiments involving animal studies were carried out according to the ethics policies and procedures approved by the Guidelines of the Animal Care and Use Committee of Southern University of Science and Technology (ethical number: AUP-220402-YCB-0189-01).

Data availability

The data reported in this paper have been deposited in the OMIX, China National Center for Bioinformation/Beijing Institute of Genomics, Chinese Academy of Sciences (https://ngdc.cncb.ac.cn/omix: accession no. OMIX1000).

Declaration of Competing Interest

The authors declare that they have no known competing financial interests or personal relationships that could have appeared to influence the work reported in this paper.

Acknowledgments

This work was supported by National Key Research and Development Program of China (2020YFA0908000 and 2022YFC2303600), National Natural Science Foundation of China (82003721, 82074098, 82274182, 81841001, 82173914), the Science and Technology Foundation of Shenzhen (Shenzhen Clinical Medical Research Center for Geriatric Diseases), Shenzhen Science and Technology Innovation Commission (JCYJ20210324114014039, JCYJ20210324115800001, JCYJ20220818102613029), Guangdong Basic and Applied Basic Research Foundation (2020A1515110549), the Innovation Team and Talents Cultivation Program of National Administration of Traditional Chinese Medicine (No: ZYYCXTD-C-202002), Guangdong-Dongguan Joint Fund Regional Cultivation Project (Grant Nos. 2021B1515140033), and Dongguan Science and Technology of Social Development Program (Grant Nos. 20221800905732), Shenzhen Governmental Sustainable Development Fund (KCXFZ20201221173612034), Shenzhen key Laboratory of Kidney Diseases (ZDSYS201504301616234), Shenzhen Fund for Guangdong Provincial High- level Clinical Key Specialties (NO.SZGSP001).

Appendix A. Supplementary material

Supplementary data to this article can be found online at https://doi.org/10.1016/j.jare.2022.12.007.

References

[1] Kenyon CJ. The genetics of ageing. Nature 2010;464(7288):504–12.
[2] Campisi J et al. From discoveries in ageing research to therapeutics for healthy ageing. Nature 2019;571(7764):183–92.
[3] Longo VD, Fabrizio P. Chronological aging in Saccharomyces cerevisiae. Subcell Biochem 2012;57:101–21.
[4] Harris ID et al. Fertility and the aging male. Reviews in urology 2011;13(4): e184–90.
[5] Frungieri MB et al. Male and female gonadal ageing: its impact on health span and life span. Mech Ageing Dev 2021;197:111519.
[6] Sharma, R., et al., *Effects of increased paternal age on sperm quality, reproductive outcome and associated epigenetic risks to offspring.* Reproductive biology and endocrinology : RB&E, 2015. **13**: p. 35-35.
[7] Zacchini F et al. Delayed parenthood and its influence on offspring health: what have we learned from the mouse model†. Biol Reprod 2022;106 (1):58–65.
[8] Jan SZ et al. Molecular control of rodent spermatogenesis. Biochim Biophys Acta 2012;1822(12):1838–50.
[9] Tan K et al. Transcriptome profiling reveals signaling conditions dictating human spermatogonia fate in vitro. Proc Natl Acad Sci U S A 2020;117 (30):17832–41.
[10] Zhang W et al. The ageing epigenome and its rejuvenation. Nat Rev Mol Cell Biol 2020;21(3):137–50.
[11] Wu H et al. Advantages of Single-Nucleus over Single-Cell RNA Sequencing of Adult Kidney: Rare Cell Types and Novel Cell States Revealed in Fibrosis. J Am Soc Nephrol 2019;30(1):23–32.
[12] He X et al. Single-cell omics in ageing: a young and growing field. Nat Metab 2020;2(4):293–302.
[13] Guo J et al. The adult human testis transcriptional cell atlas. Cell Res 2018;28 (12):1141–57.
[14] Sohni A et al. The Neonatal and Adult Human Testis Defined at the Single-Cell Level. Cell Rep 2019;26(6):1501–1517.e4.
[15] Shami AN et al. Single-Cell RNA Sequencing of Human, Macaque, and Mouse Testes Uncovers Conserved and Divergent Features of Mammalian Spermatogenesis. Dev Cell 2020;54(4):529–547.e12.
[16] Green CD et al. A Comprehensive Roadmap of Murine Spermatogenesis Defined by Single-Cell RNA-Seq. Dev Cell 2018;46(5):651–667.e10.
[17] Wang M et al. Single-Cell RNA Sequencing Analysis Reveals Sequential Cell Fate Transition during Human Spermatogenesis. Cell Stem Cell 2018;23 (4):599–614.e4.
[18] Xia S et al. A single-cell atlas of bisphenol A (BPA)-induced testicular injury in mice. Clin Transl Med 2022;12(3):e789.
[19] Ximerakis M et al. Single-cell transcriptomic profiling of the aging mouse brain. Nat Neurosci 2019;22(10):1696–708.
[20] Chu AL et al. The Power of Single-Cell Analysis for the Study of Liver Pathobiology. Hepatology 2021;73(1):437–48.
[21] Ma S et al. Single-cell transcriptomic atlas of primate cardiopulmonary aging. Cell Res 2021;31(4):415–32.
[22] Wang S et al. Single-Cell Transcriptomic Atlas of Primate Ovarian Aging. Cell 2020;180(3):585–600.e19.
[23] Uyar B et al. Single-cell analyses of aging, inflammation and senescence. Ageing Res Rev 2020;64:101156.
[24] Zhang MJ et al. Mouse aging cell atlas analysis reveals global and cell type-specific aging signatures. Elife 2021:10.
[25] Li ZJ et al. A novel peptide specifically targeting the vasculature of orthotopic colorectal cancer for imaging detection and drug delivery. J Control Release 2010;148(3):292–302.
[26] Lu L et al. Vascular-targeted TNFα improves tumor blood vessel function and enhances antitumor immunity and chemotherapy in colorectal cancer. J Control Release 2015;210:134–46.
[27] Macosko EZ et al. Highly Parallel Genome-wide Expression Profiling of Individual Cells Using Nanoliter Droplets. Cell 2015;161(5):1202–14.
[28] Butler A et al. Integrating single-cell transcriptomic data across different conditions, technologies, and species. Nat Biotechnol 2018;36(5):411–20.
[29] McGinnis CS, Murrow LM, Gartner ZJ. DoubletFinder: Doublet Detection in Single-Cell RNA Sequencing Data Using Artificial Nearest Neighbors. Cell Syst 2019;8(4):329–337.e4.
[30] Jung M et al. Unified single-cell analysis of testis gene regulation and pathology in five mouse strains. Elife 2019:8.
[31] Liberzon A et al. The Molecular Signatures Database (MSigDB) hallmark gene set collection. Cell Syst 2015;1(6):417–25.
[32] Aibar S et al. SCENIC: single-cell regulatory network inference and clustering. Nat Methods 2017;14(11):1083–6.
[33] Efremova M et al. Cell PhoneDB: inferring cell-cell communication from combined expression of multi-subunit ligand-receptor complexes. Nat Protoc 2020;15(4):1484–506.
[34] D. Galvis et al. Galvis, D., et al., *A dynamical systems model for the measurement of cellular senescence.* Journal of the Royal Society, Interface, 2019. **16**(159): p. 20190311-20190311.
[35] González-Gualda E et al. A guide to assessing cellular senescence in vitro and in vivo. Febs j 2021;288(1):56–80.
[36] Zhao H et al. The dynamic changes of Nrf2 mediated oxidative stress, DNA damage and base excision repair in testis of rats during aging. Exp Gerontol 2021;152:111460.
[37] Selvaratnam J, Robaire B. Overexpression of catalase in mice reduces age-related oxidative stress and maintains sperm production. Exp Gerontol 2016;84:12–20.
[38] Amaral S, Amaral A, Ramalho-Santos J. Aging and male reproductive function: a mitochondrial perspective. Front Biosci (Schol Ed) 2013;5:181–97.
[39] Kiss T et al. Single-cell RNA sequencing identifies senescent cerebromicrovascular endothelial cells in the aged mouse brain. Geroscience 2020;42(2):429–44.
[40] Matzkin ME et al. Hallmarks of Testicular Aging: The Challenge of Anti-Inflammatory and Antioxidant Therapies Using Natural and/or Pharmacological Compounds to Improve the Physiopathological Status of the Aged Male Gonad. Cells 2021;10(11).
[41] Huang D et al. Steroidogenesis decline accompanied with reduced antioxidation and endoplasmic reticulum stress in mice testes during ageing. Andrologia 2018;50(1).
[42] Matzkin ME et al. Alterations in oxidative, inflammatory and apoptotic events in short-lived and long-lived mice testes. Aging (Albany NY) 2016;8 (1):95–110.

[43] Frungieri MB et al. Ageing and inflammation in the male reproductive tract. Andrologia 2018;50(11):e13034.
[44] Mosser DM, Hamidzadeh K, Goncalves R. Macrophages and the maintenance of homeostasis. Cell Mol Immunol 2021;18(3):579–87.
[45] Boukouvalas A, Hensman J, Rattray M. BGP: identifying gene-specific branching dynamics from single-cell data with a branching Gaussian process. Genome Biol 2018;19(1):65.
[46] Mah LJ, El-Osta A, Karagiannis TC. gammaH2AX: a sensitive molecular marker of DNA damage and repair. Leukemia 2010;24(4):679–86.
[47] Aitken RJ, De Iuliis GN. Origins and consequences of DNA damage in male germ cells. Reprod Biomed Online 2007;14(6):727–33.
[48] Plant TM. Undifferentiated primate spermatogonia and their endocrine control. Trends Endocrinol Metab 2010;21(8):488–95.
[49] Jin S et al. Inference and analysis of cell-cell communication using Cell Chat. Nat Commun 2021;12(1):1088.
[50] Ramilowski JA et al. A draft network of ligand-receptor-mediated multicellular signalling in human. Nat Commun 2015;6:7866.
[51] Cho H et al. Nonconventional CD8+ T cell responses to Listeria infection in mice lacking MHC class Ia and H2–M3. J Immunol 2011;186(1):489–98.
[52] Kubben N et al. Repression of the Antioxidant NRF2 Pathway in Premature Aging. Cell 2016;165(6):1361–74.
[53] Finkel T, Holbrook NJ. Oxidants, oxidative stress and the biology of ageing. Nature 2000;408(6809):239–47.
[54] Schmidt JA et al. In vivo and in vitro aging is detrimental to mouse spermatogonial stem cell function. Biol Reprod 2011;84(4):698–706.
[55] Ryu BY et al. Effects of aging and niche microenvironment on spermatogonial stem cell self-renewal. Stem Cells 2006;24(6):1505–11.
[56] Liao J et al. Transcriptomic and epigenomic profiling of young and aged spermatogonial stem cells reveals molecular targets regulating differentiation. PLoS Genet 2021;17(7):e1009369.
[57] Gunes S et al. Effects of aging on the male reproductive system. J Assist Reprod Genet 2016;33(4):441–54.
[58] Kühnert B, Nieschlag E. Reproductive functions of the ageing male*. Hum Reprod Update 2004;10(4):327–39.
[59] Mogilenko DA, Shchukina I, Artyomov MN. Immune ageing at single-cell resolution. Nat Rev Immunol 2021:1–15.
[60] Giannessi F et al. Ultrastructure of testicular macrophages in aging mice. J Morphol 2005;263(1):39–46.
[61] Kimmel JC et al. Murine single-cell RNA-seq reveals cell-identity- and tissue-specific trajectories of aging. Genome Res 2019;29(12):2088–103.
[62] Zhang H et al. The landscape of regulatory genes in brain-wide neuronal phenotypes of a vertebrate brain. Elife 2021;10.
[63] Yousefzadeh MJ et al. Heterochronic parabiosis regulates the extent of cellular senescence in multiple tissues. Geroscience 2020;42(3):951–61.
[64] Hense JD et al. Senolytic treatment reverses obesity-mediated senescent cell accumulation in the ovary. Geroscience 2022;44(3):1747–59.
[65] Sun S et al. Inducible aging in Hydra oligactis implicates sexual reproduction, loss of stem cells, and genome maintenance as major pathways. Geroscience 2020;42(4):1119–32.